2006

Effect of Oblique Light Incidence on Magnetooptical Properties of One-Dimensional Photonic Crystals

Mikhail Vasiliev
Edith Cowan University

Vladimir I. Belotelov
M.V. Lomonosov Moscow State University

Andrey N. Kalish
M.V. Lomonosov Moscow State University

Vyacheslav A. Kotov
A.M. Prokhorov General Physics Institute, Moscow

Anotoly K. Zvezdin
A.M. Prokhorov General Physics Institute, Moscow

See next page for additional authors

10.1109/TMAG.2005.862765
This article was originally published as: Vasiliev, M. , Belotelov, V., Kalish, A., Kotov, V., Zvezdin, A., & Alameh, K. (2006). Effect of Oblique Light Incidence on Magnetooptical Properties of One-Dimensional Photonic Crystals. IEEE Transactions on Magnetics, 42(3), 382-388. Original article available here

Effect of Oblique Light Incidence on Magnetooptical Properties of One-Dimensional Photonic Crystals

M. Vasiliev[1], V. I. Belotelov[2], A. N. Kalish[2], V. A. Kotov[3], A. K. Zvezdin[3], and K. Alameh[1]

[1]Centre of Excellence for Microphotonic Systems (COMPS), Electron Science Research Institute, Edith Cowan University, Joondalup, WA 6027, Australia
[2]M.V. Lomonosov Moscow State University, Faculty of Physics, Moscow, Russia
[3]A.M. Prokhorov General Physics Institute, Moscow, Russia

We have investigated the magnetooptical properties of one-dimensional magnetic photonic crystals for the case of oblique light incidence. We developed a theoretical model based on the transfer matrix approach. We found several new effects such as transmittance resonance peak shift versus external magnetic field and the Faraday effect dependence on the incidence angle. We discuss several possible one-dimensional magnetic photonic crystals applications for the optical devices.

***Index Terms*—Band gap defect modes, magnetic photonic crystals, oblique incidence.**

I. Introduction

THEORETICAL and experimental studies of magnetic photonic crystal (MPC) structures have gained much attention in the past several years, largely due to the new optical properties that are inherent to such structures. We take the term MPC to imply a photonic crystal (or photonic band gap) material containing magnetic and nonmagnetic constituents. For the near-infrared frequency range corresponding, for example, to the wavelength of 1.55 μm, the most suitable magnetic materials are Bi- or Ce-substituted yttrium iron garnets. These materials possess a relatively large specific Faraday rotation of about 1 deg/μm and have a very small absorption at the wavelengths around 1.55 μm, which is of prime importance for their possible applications [1].

First works describing MPCs operating in the near infrared region appeared in 1997 [2], where random multilayered one-dimensional (1-D) photonic crystals composed of Bi-substituted YIG and nonmagnetic dielectric layers, showed up to 280 times Faraday effect enhancement in comparison to homogeneous yttrium iron garnet films. However, the transmittance of these reported MPCs was limited to about 2%.

Subsequently, several other similar one-dimensional (1-D) MPCs were considered both theoretically and experimentally [3]–[14]. Steel *et al.* in particular predicted the high transmission and large Faraday rotation for the 1-D MPC with alternating magnetic (Bi:YIG) and nonmagnetic layers of quarter-wave thicknesses with structural defects realized by omitting some layers [3]. For such a photonic structure, a Faraday rotation of 45° and a transmittance of 98% were obtained using a thickness of only 15 μm, while for a uniform magnetic medium the required propagation length is 300 μm.

During the past several years, the fabrication of two- and even three-dimensional MPC became possible and many interesting structures mainly based on artificial opals were produced [13].

While the impact of normal light incidence of 1-D magnetic photonic crystals has received substantial attention, the case of oblique incidence, which is of significant practical interest, was almost never considered.

In this paper, we investigate the optical properties of one-dimensional MPC in the case of oblique light incidence and provide the theoretical analysis of the transmittance, reflectance, and Faraday rotation spectra behavior as a function of the angle of incidence.

Apart from the study of the fundamental properties of MPC, this study is also of practical interest for several reasons. The resonant wavelength was found to change with the angle of incidence. Therefore, the optical properties of MPC can be tuned easily. The differences in the propagation characteristics between the s-wave (light polarized in a plane perpendicular to the plane of incidence) and the p-wave (polarization plane parallel to the plane of incidence) may lead to the ability to tune the polarization of transmitted light. This opens a possibility of using MPCs as polarizers. Furthermore, the investigation of the incidence angle dependencies of transmittance and reflectance is of practical interest for the development of some integrated optics devices. In addition to that, if the incident light beam is narrow, the location of the points where the reflected or transmitted beams exit the structure depends on the wavelength. Thus, a spatial separation of the spectral components of incident light can be realized, and the MPC may be used as an efficient demultiplexer.

II. Theory

Optical properties of 1-D MPCs modeling was performed on the basis of the transfer matrix technique [14].

Let us consider a 1-D MPC placed between two media: medium-1 and medium-2 of dielectric constants ε_a and ε_b, respectively (Fig. 1). The direction of z-axis is chosen normal to the interfaces of film layers. The electromagnetic wave of the wave vector $\vec{k}_0$ is incident on the front interface of the MPC first layer.

The electromagnetic field in the nth layer can be represented as a superposition of the so-called "proper modes." In the one-

Digital Object Identifier 10.1109/TMAG.2005.862765

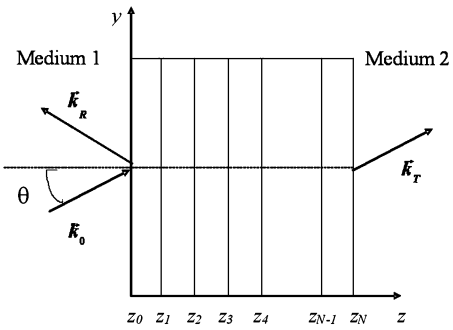

Fig. 1. Geometry of the problem.

dimensional case, the proper modes are four waves that propagate independently of each other in each of the two opposite directions and having the states of polarization which are preserved during propagation. The electric field amplitudes of proper modes at the boundary of the layer n (point z_n) are represented by a column vector A_n. The propagation of proper modes inside the nth layer is described by the propagation matrix P_n, which relates the amplitudes of proper modes on the two boundaries of the layer (i.e., at points z_n and z_{n+1}). Since the proper modes propagate independently of each other, the propagation matrix is diagonal, i.e., describes only the phase shifts. The amplitudes of the proper modes in different layers are linked by a dynamic matrix D_n that converts the vector A_n into a column vector of tangential electric and magnetic field amplitudes. The boundary conditions for the tangential components of electric and magnetic fields at the point z_{n+1} can be represented as follows:

$$D_n P_n A_n = D_{n+1} A_{n+1}. \tag{1}$$

Using (1), one can obtain a set of equations that relate the amplitudes of proper modes incident on and leaving the MPC structure:

$$A_0 = D_0^{-1} D_1 P_1^{-1} \dots D_N P_N^{-1} D_N^{-1} D_{N+1} A_{N+1}. \tag{2}$$

One of the features of the transfer matrix technique is its universality, which enables the optical properties of both periodic and nonperiodic multilayered structures to be accurately modeled.

Let YZ be the plane of incidence (Fig. 1). The proper modes obey the Fresnel equation:

$$n^2 \vec{E} - \vec{n}(\vec{n}\vec{E}) = \hat{\varepsilon}\vec{E} \tag{3}$$

where $\vec{n} = (c/\omega)\vec{k}, \vec{k}$ is the wave vector, and $\hat{\varepsilon}$ is the dielectric tensor of the medium. Since the tangential component of wave vector is continuous at all interfaces, then $n_y = \sqrt{\varepsilon_a}\sin\theta$, where θ is the angle of incidence. The component n_z is determined from the condition of solvability of the (3) with respect to the electric field components.

Dielectric tensor of an optically isotropic magnetic medium magnetized along Z-axis has the form

$$\hat{\varepsilon} = \begin{pmatrix} \varepsilon_1 & -ig & 0 \\ ig & \varepsilon_1 & 0 \\ 0 & 0 & \varepsilon_2 \end{pmatrix} \tag{4}$$

where the gyration, g, and dielectric constant, ε_2, depend on the magnetization, with g and $b = \varepsilon_2 - \varepsilon_1$ vanishing at zero magnetization. This implies that optical anisotropy for such materials is purely magnetic field-induced [1].

Using (3) and (4), one can get the following expression for the longitudinal wave number n_z in a magnetic layer magnetized along Z-axis

$$n_{z\pm}^2 = \varepsilon_1 - \frac{n_y^2}{2}\left(\frac{b+2\varepsilon_1}{b+\varepsilon_1}\right) \pm \sqrt{\frac{n_y^4}{4}\left(\frac{b}{\varepsilon_1+b}\right)^2 + g^2\left(1-\frac{n_y^2}{\varepsilon_1+b}\right)}. \tag{5}$$

The proper modes electric field components are determined from (3):

$$E_x = \frac{-ig}{n^2-\varepsilon_1}E_y, \quad E_z = \frac{n_y n_z}{n_y^2-\varepsilon_2}E_y. \tag{6}$$

Using (6), the normalized electric $\vec{e}$ and magnetic $\vec{h}$ fields of the proper modes, which are required to calculate the dynamic matrix D, can be obtained as follows:

$$\vec{e} = \vec{E}/|\vec{E}|, \quad \vec{h} = \vec{n} \times \vec{e}/|\vec{n}|. \tag{7}$$

The gyration vector g is linear with respect to the media magnetization, while the Cotton–Mouton constant b is proportional to the magnetization squared, which classifies them as being first- and second-order magnetooptical constants, respectively. For the conventional magnetooptical materials (e.g., for the yttrium iron garnets) the second-order effects can be neglected, and consequently, we restrict our consideration here to only the first order magnetooptical phenomena by setting the Cotton–Mouton constant, b, to zero. Furthermore, due to the relatively small values of the gyration, the condition $\varepsilon_1 \cos\theta_m \gg g$ is satisfied for angles θ_m smaller than 85°, where θ_m is the average angle between the Z-axis and proper mode wave vectors inside the magnetic medium. Thus, in the magnetic media, the proper modes are two elliptically polarized waves. Taking these conditions into account, expressions (5) and (6) can be simplified substantially, and the expression for the longitudinal part of the normalized wave vector can be simplified to

$$n_z = \sqrt{\varepsilon_1}\cos\theta_m \pm \frac{g}{2\sqrt{\varepsilon_1}} \tag{8}$$

and the proper mode electric field vector in Cartesian coordinates (see Fig. 1) is simply expressed as

$$\vec{E}_\pm = A \begin{pmatrix} \mp i \\ \cos\theta_m \\ -\tan\theta_m\left(\cos\theta_m \mp \frac{g}{2\varepsilon_1}\right) \end{pmatrix} \times \exp[ik_0(n_z z + n_y y - ct)] \tag{9}$$

where A is a normalization constant.

The above expression determines two elliptically polarized waves with the electric field vector circumscribing cone surfaces with the elliptical basis and opening semi-angle

$$\beta = \frac{\pi}{2} - \frac{g \sin\theta_{\rm m}}{\sqrt{2}\varepsilon_1}. \tag{10}$$

At the same time, $(g\sin\theta_{\rm m})/(\sqrt{2}\varepsilon_1) \ll 1$, and these cone surfaces are very close to planes. Consequently, to describe the Faraday effect for the oblique incidence one can ignore slight nonorthogonality of the electric field and the wave vector and consider two mutually perpendicular p and s directions, in analogy with the conventional terminology.

Providing that at the entrance into the magnetic layer the radiation was p-polarized, one can obtain for the wave function of p- and s-components defined in this way

$$\begin{pmatrix} E_p \\ E_s \end{pmatrix} = 2A \begin{pmatrix} \cos\Delta kz - i\frac{g}{2\varepsilon_1}\tan\theta_m \sin\theta_m \sin\Delta kz \\ \sin\Delta kz \end{pmatrix} \times \exp[ik_0(\bar{n}_z z + n_y y - ct)] \tag{11}$$

where $\bar{n}_z = (n_{z+} + n_{z-})/2 = \sqrt{\varepsilon_1}\cos\theta_m$, and

$$\Delta k = k_0(n_{z+} - n_{z-})/2 = \frac{gk_0}{2\sqrt{\varepsilon_1}}. \tag{12}$$

The Faraday effect is determined by the value of the phase shift between two orthogonal elliptical polarizations, which is proportional to Δk. It is worth noticing that for relatively small medium magnetization the Faraday rotation can be assumed independent of the incidence angle and hence light ellipticity can be neglected. Consequently, the change in Faraday rotation with respect to the incidence angle is mainly due to the redistribution of electromagnetic wave energy among magnetic and nonmagnetic layers.

For the nonmagnetic layers, the dielectric tensor, ε, is diagonal with equal elements. In this case $n_z^2 = \varepsilon - n_y^2$ for any state of light polarization. Since the proper modes have orthogonal polarizations, it is simpler to choose s- and p- plane polarizations as proper modes. The unit vectors of electric and magnetic fields for s- and p-polarizations of light with $k_z > 0$ are given by

$$\vec{e}_s = (1,0,0), \quad \vec{e}_p = \left(0, \frac{n_z}{\sqrt{\varepsilon}}, -\frac{n_y}{\sqrt{\varepsilon}}\right),$$
$$\vec{h}_{s,p} = \frac{\vec{n} \times \vec{e}_{s,p}}{|\vec{n}|}. \tag{13}$$

The propagation and dynamic matrices for a 1-D MPC have the forms

$$P_n = \begin{pmatrix} e^{ik_0 n_{z+} d} & 0 & 0 & 0 \\ 0 & e^{-ik_0 n_{z+} d} & 0 & 0 \\ 0 & 0 & e^{ik_0 n_{z-} d} & 0 \\ 0 & 0 & 0 & e^{-ik_0 n_{z-} d} \end{pmatrix},$$
$$D_n = \begin{pmatrix} \vec{e}_{1,+}\vec{x} & \vec{e}_{1,-}\vec{x} & \vec{e}_{2,+}\vec{x} & \vec{e}_{2,-}\vec{x} \\ n_{1,+}\vec{h}_{1,+}\vec{y} & n_{1,-}\vec{h}_{1,-}\vec{y} & n_{2,+}\vec{h}_{2,+}\vec{y} & n_{2,-}\vec{h}_{2,-}\vec{y} \\ \vec{e}_{1,+}\vec{y} & \vec{e}_{1,-}\vec{y} & \vec{e}_{2,+}\vec{y} & \vec{e}_{2,-}\vec{y} \\ n_{1,+}\vec{h}_{1,+}\vec{x} & n_{1,-}\vec{h}_{1,-}\vec{x} & n_{2,+}\vec{h}_{2+}\vec{x} & n_{2,-}\vec{h}_{2,-}\vec{x} \end{pmatrix} \tag{14}$$

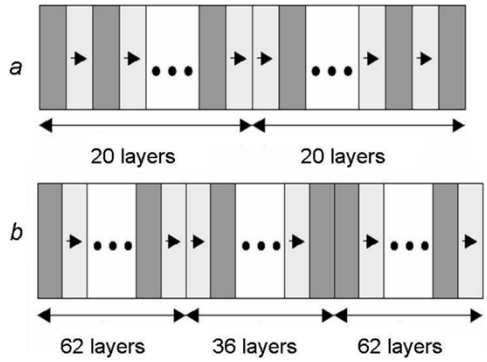

Fig. 2. Structures of $(\mathrm{NM})^{10}(\mathrm{MN})^{10}$ (a) (with one defect) and of $(\mathrm{NM})^{31}(\mathrm{MN})^{18}(\mathrm{NM})^{31}$ (b) (with two defects).

where $k_0 = (\omega/c)$, the indices "+" or "−" distinguish the directions of propagation along the z-axis, and the indices "1" or "2" denote two principal states of polarization. Using (4), (6), and (14), it is straightforward to obtain analytical expressions for the matrices P_n, and D_n in each MPC layer and relate proper modes amplitudes vectors A_0, A_{N+1} at the front and end of the MPC, respectively. Knowing the value of A_0 and A_{N+1}, the optical characteristics of reflected and transmitted light can be determined. For most of the practical implementations, light transmittance through the MPC along with the Faraday rotation angle are of prime importance. Provided that p-polarization is incident, the latter is given by [1]

$$\Phi = \frac{1}{2}\mathrm{atan}\left(\frac{2\mathrm{Re}\chi}{1-|\chi|^2}\right) \tag{15}$$

where $\chi = E_s/E_p, E_s, E_p$ are proper modes amplitudes in the medium-2.

The other crucial property of the polarized light is its ellipticity angle ξ, which can be determined by [1]

$$\xi = \frac{1}{2}\mathrm{asin}\left(\frac{2\mathrm{Im}\chi}{1+|\chi|^2}\right). \tag{16}$$

III. Results and Discussion

In this work, we investigate 1-D MPCs with structural defects realized by changes in the sequence of magnetic and nonmagnetic layers. Typical schemes of the structures are shown in Fig. 2.

The thickness of every layer is $\lambda/4\sqrt{\varepsilon_n}$, where λ is the wavelength in vacuum. The properties of the layers are chosen in such a way that material of the nonmagnetic layers is GGG (gadolinium gallium garnet) which has $\varepsilon = 3.71$ and $g = 0$, and the material of the magnetic layers is Ce:YIG (cerium-substituted yttrium iron garnet) having $\varepsilon_1 = \varepsilon_2 = 4.88$, and $g = 0.009$ [10]. Consequently, for $\lambda = 1.55$ μm the thickness of GGG-layer is around 201 nm, while the thickness of the Ce:YIG layer is around 175 nm. The surrounding media are air and glass, which have $\varepsilon_a = 1$ and $\varepsilon_b = 2.31$, respectively.

Fig. 3 shows the transmittance and Faraday rotation angle spectra for the MPC structure of formula $(\mathrm{NM})^{10}(\mathrm{MN})^{10}$ in the case of normal incidence. In this formula, N denotes a nonmagnetic layer and M denotes a magnetic layer, while the

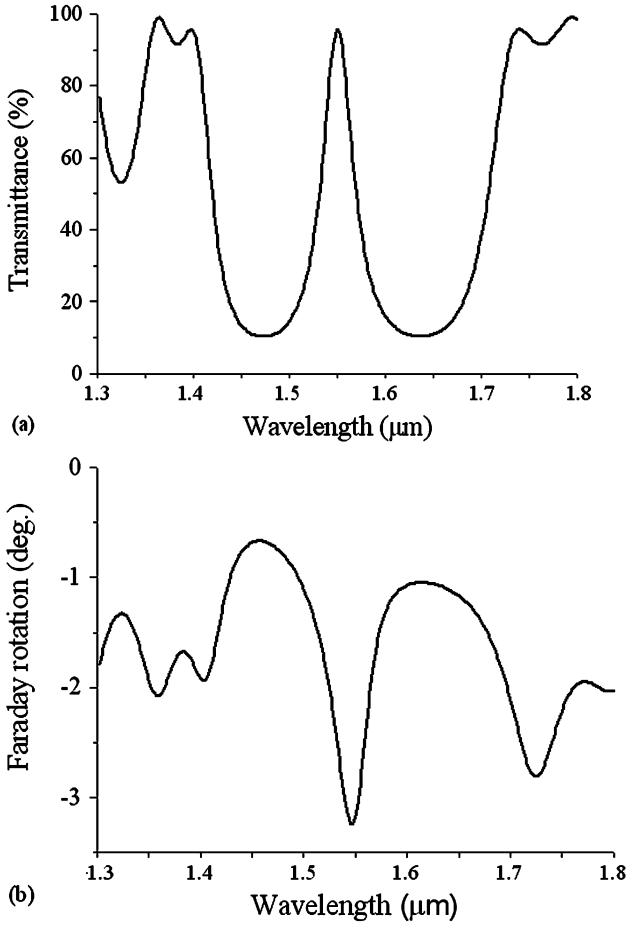

Fig. 3. Transmittance (a) and Faraday rotation angle (b) spectra for the MPC of formula $(\mathrm{NM})^{10}(\mathrm{MN})^{10}$ in the case of normal incidence.

numbers (superscripts) determine the repetition index of the corresponding sub-stacks in the MPC structure. This MPC has one structural defect that leads to a resonant transmittance peak inside its band gap ("defect mode").

This peak takes place at the design wavelength of 1.55 μm. At the same wavelength, the Faraday rotation angle also has a peak, which may be interpreted by the fact that the group velocity around the wavelength of 1.55 μm is close to zero, so that the effective time of interaction between the electromagnetic radiation and the MPC magnetization is significantly high. Two other Faraday rotation peaks appear at the edges of the band gap at the wavelengths of around 1.36 and 1.72 μm, which correspond to the group velocity vanishing effect. It is worth noticing that the Faraday rotation peak at the long-wavelength edge is higher than that at the short-wavelength edge. This is quite a general situation provided that the nonmagnetic medium refractive index is smaller than the refractive index of the magnetic constituent. This is due to the fact that the electromagnetic field energy at the long-wavelength edge of the photonic band gap is mainly located inside the higher refractive index medium, which is the magnetic one for this case.

At normal incidence the p- and s- polarizations are equivalent, but this is not the case for the oblique incidence. The difference appears even for the light coming onto the interface between two semi-infinite materials. For example, if the angle of incidence

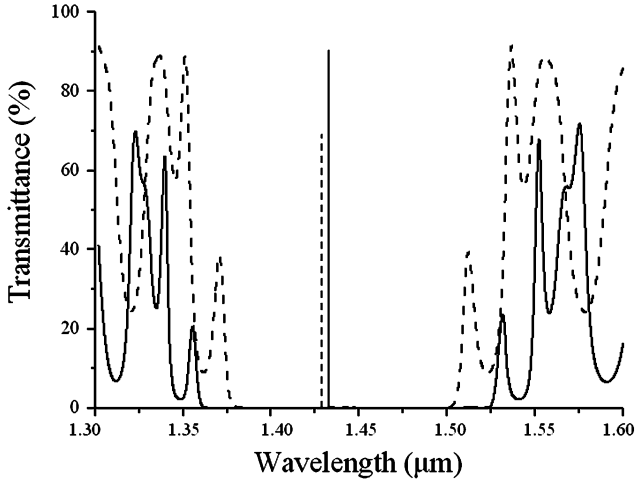

Fig. 4. Transmittance spectra for the MPC of formula $(\mathrm{NM})^{31}(\mathrm{MN})^{18}(\mathrm{NM})^{31}$ at the 50° incidence angle for two basic incident polarizations: s- (solid line) and p- (dashed line).

equals to the Brewster angle then p-polarization does not reflect and transmits fully while s-polarization continues to reflect and transmit partially. These differences are much more pronounced for the multilayered stacks, i.e., in 1-D photonic crystals. Thus, s- and p-waves of some frequencies in 1-D photonic crystals can have absolutely different transmittance: almost 100% for p-wave and almost zero percent for s-wave, or vice versa. Such effect is widely used for interference optical polarizers.

Due to the magnetooptical effects, MPC structures can be used as tunable optical devices. This can be accomplished by two approaches, namely: 1) the presence of the Faraday effect inside MPCs allows for the substantial polarization rotation, which depends on whether s- or p-wave is incident and 2) magnetooptical light-medium interaction leads to the changes in s- and p-waves transmittance spectra.

While modeling the MPCs optical properties, we have found that they are considerably influenced by the magnetic field at the defect mode frequencies rather than at the band gaps' edges. That is why the emphasis was made exactly at the defect levels inside the band gaps.

Fig. 4 demonstrates transmittance for the MPC of formula $(\mathrm{NM})^{31}(\mathrm{MN})^{18}(\mathrm{NM})^{31}$ at the 50° incidence angle. It can be seen that the transmittance spectra for two main polarizations vary appreciably. Namely, the band gap width for s-wave (solid line) is about 30% wider, which leads to some frequencies of simultaneously zero transmittance for s-wave and approximately 40% transmittance for p-wave (dashed line). Defect modes of both polarizations are also recognizable. Although the peak shift of the p-wave defect mode transmittance from the peak transmittance of the s-wave is only 2 nm, some other MPC structures can be found that have a more pronounced shift.

Medium magnetization also affects the peaks position, as shown in Fig. 5 where transmittance peaks of the incident p-wave for $g = 0, g = 0.01, g = 0.03$, and $g = 0.05$ are plotted. The peak shift is proportional to the medium gyration, and, consequently, to the medium magnetization. The linear shift in the defect mode position has the same nature as the magnetic field induced shift of the band gap edges theoretically

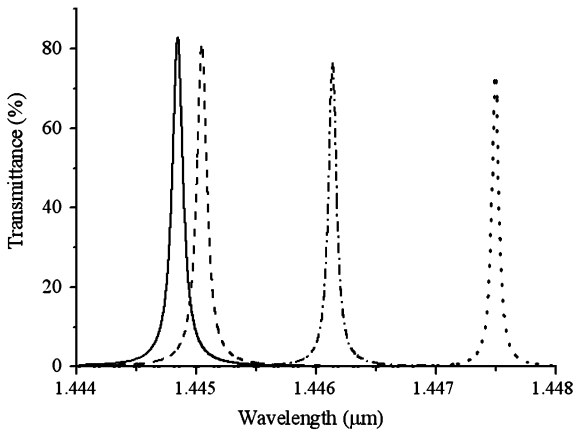

Fig. 5. Transmittance peak position of the p-polarization incident on the MPC of formula $(\mathrm{NM})^{31}(\mathrm{MN})^{18}(\mathrm{NM})^{31}$ at the 50° angle for four different magnetic layers gyrations: $g = 0$ (solid line), $g = 0.01$ (dashed line), $g = 0.03$ (dash-dotted line), and $g = 0.05$ (dotted line).

predicted and explained in [12]. It is worth noticing that the peaks of different polarization (s-polarization for the considered case) generally occur at different frequencies. That is why the effect described here is of practical value because it can be utilized for tunable optical devices such as polarizers and shutters. The latter, for example, being organized on the basis of the suggested structures will enable to separate s- and p-incident polarizations at the desired wavelength which can be finely tuned by the magnetic field.

While MPCs have been proposed for optical polarizers, the output light ellipticity can significantly limit the performance of MPC-based polarizers. In the case of the discussed MPC scheme the ellipticity ξ increases with the gyration and it is about 1.5° for the Ce:YIG saturation magnetization corresponding to $g = 0.009$. Consequently, for the best performances, optimization of the MPC structure is vital.

We have considered an MPC structure with many layers that lead to ultra-narrow transmission resonances. At the same time, the Faraday rotation spectrum also has peaks but they occur at almost zero transmittance, so for applications where polarization plane rotation is needed some other MPC structures should be found. For example, let us discuss the magnetooptical properties of one-defect MPC of formula $(\mathrm{NM})^{20}(\mathrm{MN})^{20}$, whose Faraday rotation spectra are shown in Fig. 6(a). At normal incidence the Faraday rotation for s-wave is 38° [solid line in Fig. 6(a)], having a maximum at 1.55 μm, which coincides with a high transmittance region. At the same time, for oblique incidence (incidence angle is, e.g., 63°) it is 14° higher [dashed line in Fig. 6(a)] and again has a maximum that coincides with the maximum of transmittance at around 1.40 μm. The difference in resonance positions is due to the changes in the light propagation path inside the layers, which result from the changes in the incidence angle. The Faraday rotation angle at the resonance frequency inside the band gap versus incidence angle impinging on the given structure is shown in Fig. 6(b). The transmittance at the given peaks is practically independent of the incidence angle, unless in the case of almost tangent (grazing) incidence. For the chosen MPC structure the Faraday rotation demonstrates

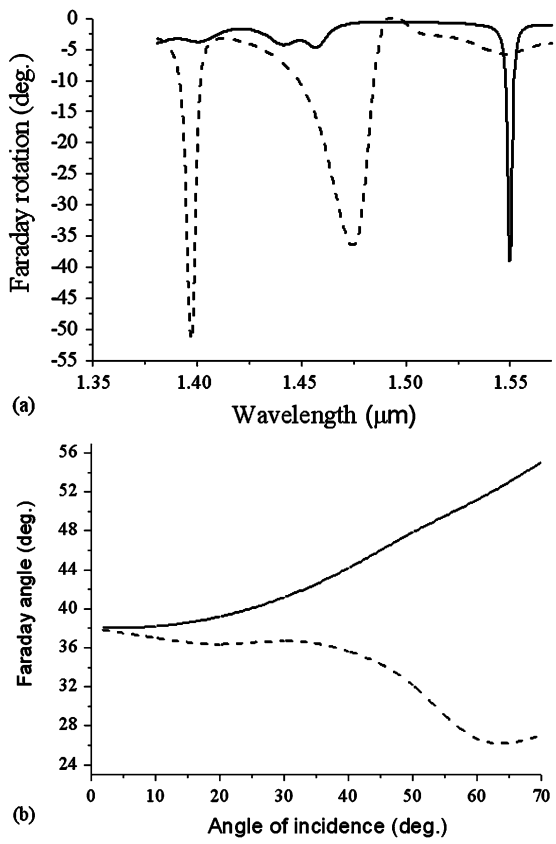

Fig. 6. Faraday rotation for the MPC of formula $(\mathrm{NM})^{20}(\mathrm{MN})^{20}$. (a) Faraday rotation spectra for the s- polarization at normal (solid line) and oblique (incidence angle is 63°) (dashed line) incidence. (b) Faraday rotation for s- (solid line) and p-polarizations (dashed line) at the peaks versus incidence angle.

an increase for the s-wave and a decrease for the p-wave with the angle of incidence. This behavior is not universal and for some other MPC structures can be opposite. In any case for a given gyration $(g = 0.009)$ the increase or decrease in the Faraday rotation does not exceed the value of several degrees per 10° of the incidence angle.

The ability to tune the operational wavelength of the MPC by varying the angle of incidence opens up a possibility of designing demultiplexers with magnetooptic equalization of transmission loss. A passive or reconfigurable (based on a spatial light modulator utilizing liquid crystal on silicon (LCOS) technology) diffraction grating can be used to generate an appropriate (peak transmission-tuned) array of incidence angles for the light carrying several WDM signal channels [15]. The light incident on the MPC has to be polarized (in an arbitrary plane for the case of near-normal incidence, since the s- and p-polarization responses in both transmission and Faraday rotation are then nearly identical). Another polarizer (analyzer) can be used in the optical path after the MPC to achieve extinction when the plane of polarization is rotated magnetooptically by 45° in a chosen direction. The transmitted intensity in each channel can then be controlled independently by rotating the required planes of polarization by $\pm 45^{\circ}$ with magnetic fields applied locally using an array of integrated current-carrying coils encircling the propagation paths of light. The crosstalk in the output

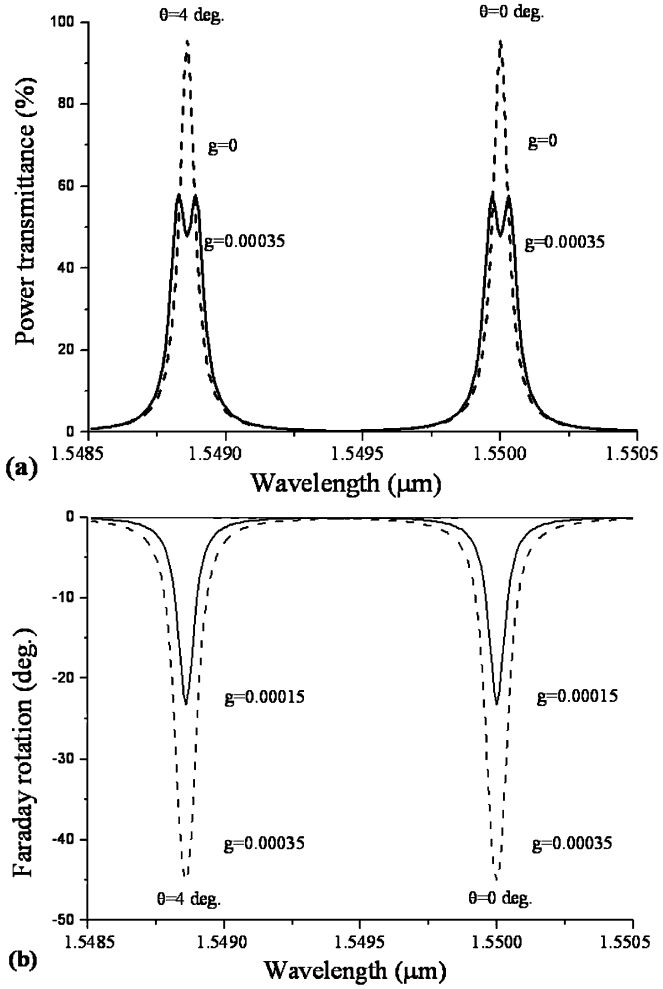

Fig. 7. Transmittance and Faraday rotation spectra of the structure $(\mathrm{NM})^{12}(\mathrm{MN})^{1}(\mathrm{NM})^{1}(\mathrm{MN})^{12}$ at normal and 4° incidence with various strengths of the applied magnetic field. (a) Averaged (unpolarized) transmittance spectra at normal and 4° incidence and their variation with gyration. (b) Faraday rotation spectra for p-component at normal and 4° incidence at various gyrations. The spectral responses of s- and p-components of polarization are almost identical at near normal incidence. $\varepsilon_a = 1, \varepsilon_b = 2.310$.

will be very low due to the spatial separation of the channel propagation paths and the spectral sharpness of the MPC transmission resonances which are tuned to their corresponding angles of incidence. Due to the very low absorption of bismuth or cerium-substituted YIG in the 1.55 μm optical telecommunications window, it is possible to design MPC structures possessing very sharp spectral resonances having high transmission coupled with significantly enhanced Faraday rotation. In this case, relatively small magnetic fields can achieve large Faraday rotations within narrow spectral windows, which can be tuned by changing the incidence angle. For example, an MPC structure with a design formula $(\mathrm{NM})^{12}(\mathrm{MN})^{1}(\mathrm{NM})^{1}(\mathrm{MN})^{12}$, in which SiO_2-layers are used for nonmagnetic constituent ($\varepsilon = 2.24$), has a very sharp resonant behavior in both transmission and Faraday rotation near the wavelength of 1.55 μm. This quarter-wave stack structure is composed of 52 layers and has a thickness of 11.29 μm. The spectral response of this structure, its variation with the angle of incidence, and its optical response to the gyration are shown in Fig. 7. Here, we assumed two types

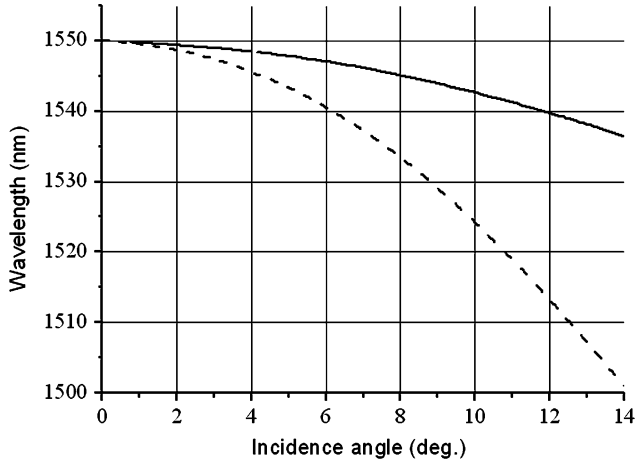

Fig. 8. MPC operational wavelength as a function of incidence angle for the structure $(\mathrm{NM})^{12}(\mathrm{MN})^{1}(\mathrm{NM})^{1}(\mathrm{MN})^{12}$ sandwiched between (i) air and glass ($\varepsilon_a = 1, \varepsilon_b = 2.310$) (solid line), or (ii) two identical media index-matched to the mean refractive index of the structure ($\varepsilon_a = \varepsilon_b = 3.168$) (dashed line).

of the surrounding media pairs, namely: 1) air and glass as before ($\varepsilon_a = 1, \varepsilon_b = 2.310$) and 2) the substrate and the exit medium which are index-matched to the mean refractive index of the structure ($\varepsilon_a = \varepsilon_b = 3.168$). The gyration required for achieving the 45° of rotation is $g = 0.00035$, which can be achieved at about 3.8% of the saturation magnetization for Ce:YIG.

The splitting of two opposite elliptical polarizations resonances and its associated reduction in peak transmission observed at high levels of induced gyration limit the dynamic range of the device and introduce some extra loss, however, in some equalizer applications these drawbacks can be outweighed by the advantages of the high-speed operation characteristic of the magnetooptic devices. The response time required for switching of each channel from a minimum to a maximum of transmitted intensity can be as short as tens of nanoseconds. The range of incidence angles (and, consequently the number of channels that can be processed by a single device of this type) can in principle be extended to large angles if control of the polarization of incident light is implemented.

The wavelength-tuning curve (the dependency of the MPC operational wavelength on the angle of incidence) of the structure being considered is shown in Fig. 8. This dependency is highly nonlinear for very small angles of incidence, but for moderate incidence angles, it can be approximated by a linear function with a slope of about 1 nm/deg for index-unmatched air and glass surrounding media and 6.7 nm/deg for index-matched surrounding media.

The structure of the dispersion grating to be used for demultiplexing the multichannel optical input must be optimized to closely match its angular dispersion function with a selected section of the wavelength-tuning curve of the MPC.

IV. Conclusion

In this paper, we have considered the case of oblique incidence of the electromagnetic radiation on 1-D MPC structures formed by alternating magnetic and nonmagnetic layers with

one or several structural defects. Such structures have an additional resonant transmittance peak inside the photonic band gap.

Theoretical analysis was based on the 4×4 transfer matrix formalism adapted to the arbitrary angle of incidence. Analytical expressions for the refractive indices (or normalized wave vector components) of proper modes inside a magnetic medium have also been derived.

To the knowledge of the authors, we have shown for the first time ever that in the case of oblique incidence the s- and p-polarizations have different transmittance resonance peaks which can be affected by the changes in the medium magnetization, and that, the transmittance maxima for two main incident polarizations are shifted with respect to each other (by several nanometers) and their bandwidth can be very narrow (about tenths or even hundredths of nanometer depending on the MPC structure), if lying in the band gap. This makes MPCs attractive for optical filtering and sensing applications.

The Faraday rotation angle of an MPC structure depends on the incident angle and can be increased with it by several tens of percent leaving the transmittance level of almost the same value. This effect is also of practical importance.

As the incidence angle increases the MPC operational wavelength decreases, which can be used to design WDM demultiplexers with magnetooptic transmission loss equalization. Such a possibility has been discussed in the paper.

Although many accompanying factors must be taken into account for practical implementation of the proposed structures, the concepts presented in this paper are very promising for many applications.

ACKNOWLEDGMENT

This work was supported by RFBR (no. 05-02-17308-a, 05-02-17064-a, 03-02-16980-a) and the Office of Science and Innovation, Western Australian Government.

REFERENCES

[1] A. Zvezdin and V. Kotov, *Modern Magnetooptics and Magnetooptical Materials*. Philadelphia, PA: IOP Publishing, 1997.

[2] M. Inoue and T. Fujii, "Magnetooptical properties of one-dimensional photonic crystals composed of random magnetic and dielectric layers," *J. Appl. Phys.*, vol. 81, pp. 5659–5665, 1997.

[3] M. J. Steel, M. Levy, and R. M. Osgood, "High transmission enhanced Faraday rotation in one-dimensional photonic crystals with defects," *IEEE Photon. Technol. Lett.*, vol. 12, no. 9, pp. 1171–1173, Sep. 2000.

[4] H. Kato, T. Matsushita, and A. Takayama, "Effect of optical losses on optical and magneto-optical properties of one-dimensional magnetophotonic crystals for use in optical isolator devices," *J. Appl. Phys.*, vol. 93, pp. 3906–3911, 2003.

[5] A. Figotin and I. Vitebsky, "Nonreciprocal magnetic photonic crystals," *Phys. Rev. E*, vol. 63, p. 066 609, 2001.

[6] H. Kato *et al.*, "Effect of optical losses on optical and magneto-optical properties of one-dimensional magnetophotonic crystals for use in optical isolator devices," *Opt. Commun.*, vol. 219, pp. 271–276, 2003.

[7] M. Inoue, K. Arai, T. Fujii, and M. Abe, "Magnetooptical properties of one-dimensional photonic crystals composed of magnetic and dielectric layers," *J. Appl. Phys.*, vol. 85, pp. 5768–5777, 1999.

[8] S. N. Kurilkina and M. V. Shuba, "Propagation and transformation of the light waves in magnetoactive periodic structures," *Opt. Spectrosc.*, vol. 93, pp. 918–923, 2002.

[9] Y. Saado, M. Golosovsky, D. Davidov, and A. Frenkel, "Tunable photonic bandgap in self-assembled clusters of floating magnetic particles," *Phys. Rev. B*, vol. 66, p. 195 108, 2002.

[10] M. Levy, H. C. Yang, M. J. Steel, and J. Fujita, "Flat-top response in one-dimensional magnetic photonic bandgap structures with Faraday rotation enhancement," *J. Lightwave Technol.*, vol. 19, no. 12, pp. 1964–1969, Dec. 2001.

[11] E. Takeda *et al.*, "Faraday effect enhancement in Co-ferrite layer incorporated into one-dimensional photonic crystal working as a Fabry-Perot resonator," *J. Appl. Phys.*, vol. 87, pp. 6782–6784, 2000.

[12] A. K. Zvezdin and V. I. Belotelov, "Magnetooptical properties of photonic crystals," *Eur. Phys. J. B*, vol. 37, pp. 479–487, 2004.

[13] I. L. Lyubchanskii, N. N. Dadoenkova, M. I. Lyubchanskii, E. A. Shapovalov, and Th. Rasing, "Magnetic photonic crystals," *J. Phys. D, Appl. Phys.*, vol. 36, pp. R277–287, 2003.

[14] V. I. Belotelov and A. K. Zvezdin, "Magneto-optical properties of photonic crystals," *J. Opt. Soc. Amer. B*, vol. 22, p. 286, 2005.

[15] S. Ahderom, M. Raisi, K. E. Alameh, and K. Eshraghian, "Dynamic WDM equalizer using opto-VLSI beam processing," *IEEE Photon. Technol. Lett.*, vol. 15, no. 11, pp. 1603–1605, Nov. 2003.

Manuscript received August 26, 2005; revised November 30, 2005 (e-mail: m.vasiliev@ecu.edu.au).